Direct observation of ordered trimers on Si(111)$\sqrt{3}\times\sqrt{3}$ $R30°$-Au by scanned-energy glancing-angle Kikuchi electron wave-front reconstruction

I. H. Hong, D. K. Liao, and Y. C. Chou
Department of Physics and Material Science Center, National Tsing-Hua University, Hsinchu, Taiwan 30043, Republic of China

C. M. Wei
Institute of Physics, Academia Sinica, Nankang, Taipei, Taiwan 11529, Republic of China

S. Y. Tong
Department of Physics, The University of Hong Kong, Pokfulam Road, Hong Kong
and Department of Physics and Laboratory for Surface Studies, University of Wisconsin–Milwaukee, Milwaukee, Wisconsin 53201

(Received 20 March 1995)

We report the first atomically resolved images of ordered Au trimers on Si(111)$\sqrt{3}\times\sqrt{3}R30°$-Au using wave-front reconstruction of scanned-energy glancing-angle Kikuchi electron spectra. Each Au image has a resolution (full width at half magnitude) of less than 1 Å . The images indicate that Au trimers are ordered and nonrotated within the surface plane and with respect to the second-layer Si plane providing direct evidence of the conjugate honeycomb-chained-trimer model for the Au-$\sqrt{3}$ system. [S0163-1829(96)07823-X]

The $\sqrt{3}\times\sqrt{3}$ $R30°$ (henceforth $\sqrt{3}$) structures of noble metals Ag and Au on Si(111) have been the subject of particularly intense studies because of the complexity of the atomic arrangements at the interface.[1] In each case, the adsorption of the metal atoms induces extensive surface restructuring—the top-layer Si atoms are completely peeled off and replaced by the metal atoms. The $\sqrt{3}$ periodicity is formed by subsequent rebonding of the metal atoms with Si atoms in the layer below.[2–4] Here, the two metal systems follow different paths: As explained by Ding, Chen, and Ho,[5] in the Au-$\sqrt{3}$ system, the Au-Au bond is stronger than either the Au-Si or Si-Si bond. This results in Au trimerization in the surface layer and the Si lattice below distorts to bond to the Au trimers (see Fig. 1). The situation is reversed for the Ag-$\sqrt{3}$ system, where the Si-Si bond is stronger than either the Ag-Si or Ag-Ag bond. Here, the Si atoms in the second layer trimerize and the Ag atoms are bonded to the remaining dangling bonds on the Si trimers.[3] The structures of the two metal-semiconductor systems, known respectively as the honeycomb-chained-trimer (HCT) and conjugate honeycomb-chained-trimer (CHCT) models for Ag-$\sqrt{3}$ and Au-$\sqrt{3}$, are supported by results of first principles total-energy calculations,[3,5] low-energy electron diffraction (LEED),[6,7] x-ray diffraction,[8] and a host of other surface characterization techniques.[4,9–12]

The Au-Au bond length in the trimers of the Au$\sqrt{3}$ system is 2.81 Å . Because Au is a strong scatterer and the trimers are on the surface layer, they should be good candidates for direct imaging. Surprisingly, to date, no imaging technique has successfully resolved individual atoms in the Au trimer. Scanning tunneling microscopy (STM) pictures of the Au-$\sqrt{3}$ system show one maximum per unit cell.[13–16] Simulation predicts that the maximum corresponds to the center of a Au trimer. Unfortunately, this is the case for both filled and empty states,[5] therefore, individual atoms in the Au trimers can never be resolved by STM. In this paper, we present the first atomically resolved images of Au atoms in the trimers of the Au-$\sqrt{3}$ system. Each Au image has a resolution (full width at half magnitude) of less than 1-Å . The images are obtained by wave-front reconstruction of scanned-energy glancing-angle Kikuchi electron spectra. Besides images of atoms within each trimer, we also obtain images of atoms in neighboring trimers. As will be shown in this paper, the latter provides direct evidence that the Au trimers are ordered and nonrotated.

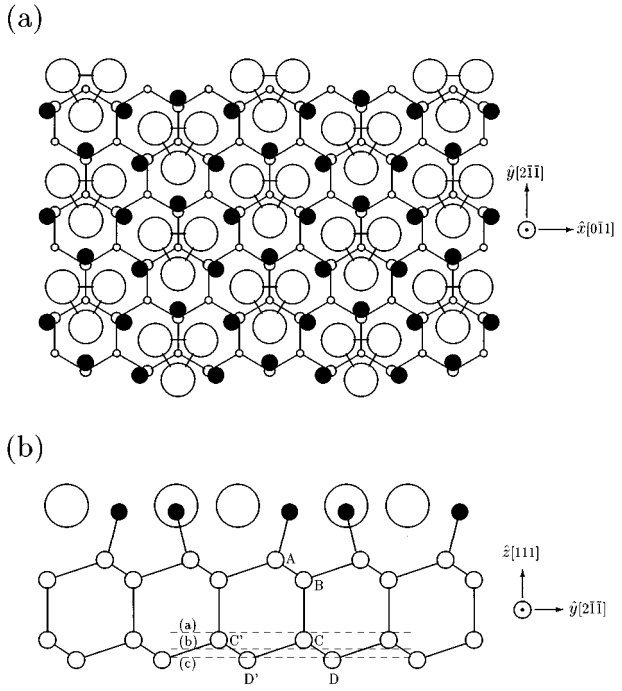

FIG. 1. Schematic (a) top view and (b) side of the CHCT model for Si(111)-$\sqrt{3}$-Au. The largest circles in (a) and (b) represent Au atoms. All other circles represent Si atoms.

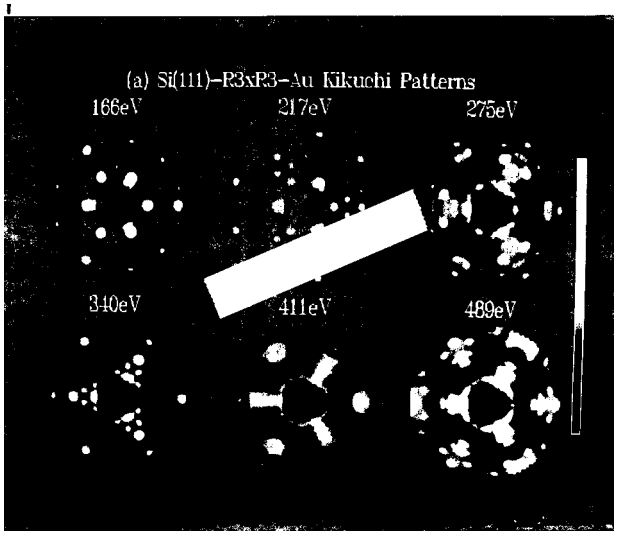

FIG. 2. Six Kikuchi patterns displayed in orthographic projection. Each pattern is threefold-symmetry averaged. The angular opening is 104°.

Because we obtain the real-space information (atomic images) by wave-front reconstruction of reciprocal-space spectra, this process allows a precise correlation between k-space patterns and real-space structure. The Au coverage is carefully monitored until a sharp $\sqrt{3}$ LEED pattern is obtained. We further measure the LEED IV spectra and compare them with published results (see below). The wave-front reconstruction of Kikuchi electron spectra is carried out at this coverage. This precise correlation between LEED patterns (sensitive to the long-range order) and real-space images (sensitive to the local order) is particularly useful in this case because recent STM studies show that at quoted 1-ML or higher Au coverages, the periodicity is 6×6 and not $\sqrt{3}$.[15–17] STM also observes that at 1-ML or higher coverages, considerable amounts of defects in the form of domain walls are present on the surface.[15,16] Both STM and x-ray diffraction studies find that the $\sqrt{3}$ phase corresponds to a Au coverage of 0.8 ML or less.[10,15,16] This has led to the speculation that perhaps a different model with only $\frac{2}{3}$ ML of Au atoms is required to explain the $\sqrt{3}$ structure. Our result directly rules out this possibility. We confirm that at a Au coverage corresponding to very sharp $\sqrt{3}$ LEED spots and below the transition to the 6×6 periodicity, the real-space arrangement consists of ordered Au trimers in accordance with the CHCT model.[5]

The experiments are carried out in a μ-metal UHV analyzing chamber (base pressure below 3×10^{-10} Torr) equipped with a three-grid rear-view LEED optics. The Si(111) substrate is cut from an n-type commercial wafer.

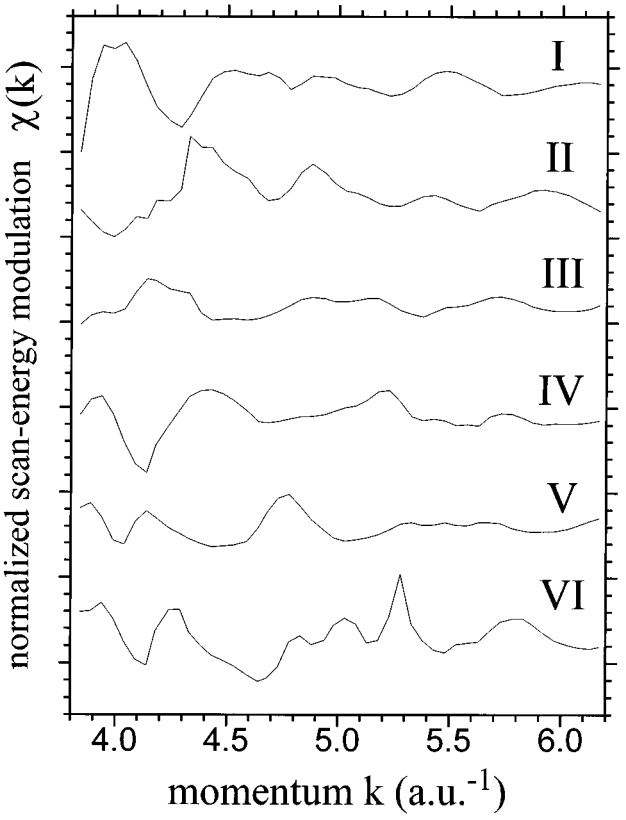

FIG. 3. The normalized intensity modulations of Kikuchi electrons at I, $\phi=45°$, $\theta=32.5°$; II, $\phi=37.5°$, $\theta=35°$; III, $\phi=30°$, $\theta=37.5°$; IV, $\phi=20°$, $\theta=22.5°$; V, $\phi=5°$, $\theta=37.5°$; VI, $\phi=0°$, $\theta=17.5°$.

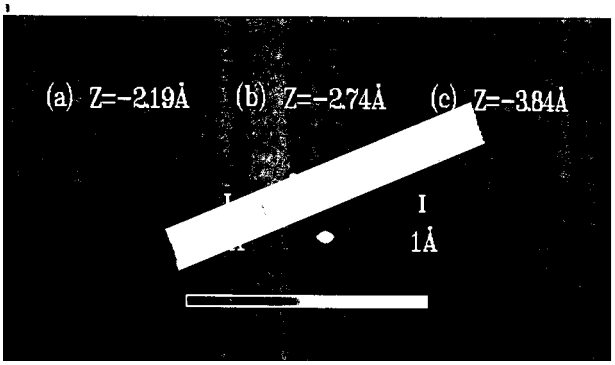

FIG. 4. Atomic images reconstructed from normal incidence Kikuchi electron patterns. The images are viewed in planes (a), (b), and (c), respectively, of Fig. 1(b).

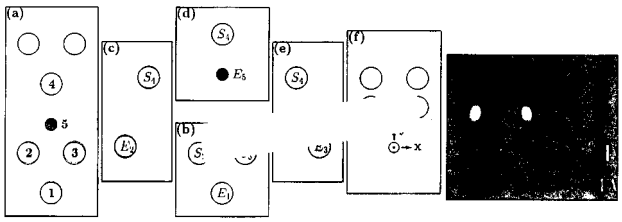

FIG. 5. Illustration of expected atomic images from glancing-angle Kikuchi electron wave-front reconstruction. The incident beam travels from bottom to top. (a) Top view of Au trimer (labeled 1, 2, and 3) and its nearest-neighbor trimer; panels (b) to (e): emitter-scatterer pairs which contribute to the hologram. (f) The expected atomic images from all inequivalent emitter-scatterer pairs. The color photograph on the right shows the images by inverting data.

Sharp 7×7 LEED patterns are obtained after repeated sputtering-annealing cycles. Gold is evaporated at room temperature and a sharp $\sqrt{3}$ pattern is obtained after annealing at 700 °C for about 10 min and slowly cooled. The coverage of Au is estimated to be slightly below 1 ML, consistent with earlier works. We measure the LEED *IV* spectra of the $\sqrt{3}$ surface and find them in excellent agreement with the published results of Quinn, Jona, and Marcus.[7] Kikuchi patterns with the incident beam normal, and 30°, 80° from normal with its parallel component pointed towards the [211] direction, and 70° from normal with its parallel component towards the [211] direction are recorded with a frame-transfer charge-coupled device camera (12-bit digitized readout, 1024×1024 pixels) coupled with an optical lens ($f/0.85$). The patterns of the fifteen different runs are averaged in real time to improve the signal to noise ratio. The electron-beam energies are varied from 120 to 700 eV. The suppressor voltage used in these experiments is 12 eV. The entire 64-energy experiment takes less than 40 min.

The Kikuchi electron patterns are inverted using the integral-energy phase-summing method (IEPSM) to eliminate multiple scattering contributions.[18–23] The inversion produces atomic images which represent vectorial atomic positions of near-neighbor atoms measured from reference atoms. The information is averaged over all equivalent reference atoms. We first show the normal incidence data and their inversion of the Au-$\sqrt{3}$ system. Figure 2 displays six Kikuchi patterns taken at different incident energies. The polar angular range is 10° to 52° due to constraint of the LEED optics. Diffraction features in the patterns exhibit a strong energy dependence. For inversion, a total of 48 patterns with energies ranging from 196 to 514 eV are used. The intensity is first normalized and plotted as a function of wave number. We show in Fig. 3 six such scanned-energy (wave-number) normalized modulations $\chi(\mathbf{k}_f)$. The normalization and inversion follow the procedure set forth in the integral-energy phase-summing method.[18–23] In the 300-eV or so energy range used, backscattering modulations which have shorter wavelengths dominate the diffraction features.[20–25] At normal incidence, we expect to observe only Si atoms at bulk sites. Figure 4 shows the reconstructed images viewed in three planes parallel to the surface. These are (a) a plane 2.19 Å from the origin. Referring to the bottom diagram of Fig. 1, this plane passes through from above the finite-sized image of atom *C*, with *B* as the reference atom (or other equivalent pairs); (b) a plane 2.74 Å from the origin, which again passes through the image of atom *C*, with *B* as the reference (or other equivalent pairs). The same plane also passes through the images of atoms *D*, *D*′, . . . , arranged in an upside-down triangle, with *B* as the reference atom, or *D*, *D*′, . . . , arranged in an upright triangle, with *A* as the reference atom (or other equivalent groups). The seven highly resolved spots, each corresponding to a single atom, are clearly seen in this figure. Finally, (c) shows a plane 3.84 Å from the origin that passes through atoms *D*, *D*′, . . . , arranged in an upright triangle, with *A* as the reference atom (or other equivalent groups). All the images are free from artifacts, and correspond to Si atoms arranged in a bulk (111) lattice.

To image the Au atoms, thought to be on the surface, we must use a grazing-incidence-beam–backscattering detection geometry. We rotate the crystal so that the LEED gun is pointed along the [211] direction at 80° from the surface normal. In this scattering geometry, the majority of the collected Kikuchi electrons come from backscattering within the first two layers of the sample. Also, the much stronger scattering factor of Au compared to Si further enhances the contribution from the Au layer. In Fig. 5(a), we show a Au trimer (atoms labeled 1, 2, and 3) and its nearest-neighbor trimer in the CHCT model. Atom 5 is a second-layer Si atom, 0.46 Å below the plane of Au atoms.[6] In Kikuchi electron imaging, every atom acts as a reference atom. Figure 5(b) shows E_1 one as the reference atom, from which the nearest-neighbor atoms S_2 and S_3 are imaged by backscattering. Similarly, Figs. 5(c) and 5(e) show atom $E_2(E_3)$ as the reference atom, imaging atom S_4 in the next trimer. From LEED, this next-nearest-neighbor Au-Au distance is 4.44 Å.[6] Figure 5(d) shows the second-layer Si atom E_5 imaging Au atom S_4. Translation of the four reference atoms to a common origin results in a predicted image depicted in Fig. 5(f), *if the CHCT model is correct*. The color figure on the right is the actual image obtained by reconstructing 32 grazing incidence (80° from normal) Kikuchi electron patterns in the energy range 196 to 389 eV. Referring to the color figure, the two brightest spots 2.78 Å from the origin are Au atoms in the same trimer. Their positions are shifted (due to a phase shift induced by the scattering factor[26,27]) by less than 0.03 Å from the LEED determined value.[6] The two furthest spots 4.43 Å away [LEED result: 4.44 Å (Ref. 6)] are equally well resolved and free from streaking. This is direct evidence that the Au trimers are mostly well ordered. Further evidence of ordered trimers on the surface is the sharp spot 2.40 Å due north of the origin. According to Fig. 5(d), this spot is the image of Au atom 4 seen from the second-layer Si atom 5. The isotropic shape of the image and the lack of streakiness of the spot suggest that the Au trimers are well ordered with respect to the second-layer Si plane. In the grazing-incidence backscattering geometry, only scatterers lying to the far side of a reference atom from the electron gun are imaged. Also, with a Au atom as the reference atom, both first and second neighbors are imaged. With the second-layer Si atom $E5$ as reference, only its nearest neighbor is imaged.

In conclusion, we have shown that inversion of scanned-energy, glancing-angle Kikuchi electron spectra produces direct evidence that ordered Au trimers are arranged in the CHCT configuration for the Au-$\sqrt{3}$ system. The Kikuchi electron spectra are measured at a coverage where the $\sqrt{3}$ LEED spots are the sharpest. The Au coverage is estimated to be slightly below 1 ML. As shown by recent STM work, there is a sizable amount of domain walls at this coverage.[15–17] From the LEED spots, the Au trimers within a domain and among different domains must have a good long-range order. Surprisingly, the best long-range order of the Au trimers is not at a lower coverage (below 0.8 ML) where STM detects few domain walls.[1] The role of the domain walls in enhancing the long-range order and reducing the total energy of this surface remains unsolved.

In Kikuchi electron spectra inversion, both surface and bulk information can be obtained by changing the angle of

incidence. Kikuchi electron patterns are easily collected using laboratory-based equipment and data acquisition takes only a few seconds per pattern. The Au-$\sqrt{3}$ system is an example where the superior resolution of the method allows an unambiguous interpretation of the images even in the presence of multiple, inequivalent reference atoms.

Y.C.C. and C.M.W. acknowledge the support of the National Science Council, Republic of China under Grant No. NSC-84-2112-M-001-006 and No. NSC-82-0208-M-007-111; S.Y.T. acknowledges support from the University of Hong Kong and NSF Grant No. DMR-9214054 and ONR Grant No. N00014-90-J-1749.

[1] See, for example, an excellent review by J. Nogami, Surf. Rev. Lett. **1**, 395 (1994), and references therein.
[2] T. Takahashi, S. Nakatani, N. Okamoto, T. Ishikawa, and S. Kikuta, Jpn. J. Appl. Phys. **27**, L753 (1988).
[3] Y. G. Ding, C. T. Chan, and K. M. Ho, Phys. Rev. Lett. **67**, 1454 (1991).
[4] S. Watanabe, M. Aono, and M. Tsukada, Phys. Rev. B **44**, 8330 (1991).
[5] Y. G. Ding, C. T. Chen, and K. M. Ho, Surf. Sci. **275**, L691 (1992).
[6] H. Over, H. Huang, S. Y. Tong, W. C. Fan, and A. Ignatiev, Phys. Rev. B **48**, 15 353 (1993).
[7] J. Quinn, F. Jona, and P. M. Marcus, Phys. Rev. B **46**, 7288 (1992).
[8] D. Dornisch, W. Moritz, H. Schultz, R. Freidenhans'l, M. Neilsen, F. Grey, and R. L. Johnson, Phys. Rev. B **44**, 11 221 (1991).
[9] E. Vlieg, E. Fontes, and J. R. Patel, Phys. Rev. B **43**, 7185 (1991).
[10] M. Chester and T. Gustafsson, Surf. Sci. **256**, 135 (1991).
[11] K. J. Wan, X. F. Lin, and J. Nogami, Phys. Rev. B **45**, 9509 (1992).
[12] A. Ichimiya, S. Kohmoto, T. Fujii, and Y. Horio, Appl. Surf. Sci. **41**/**42**, 82 (1989).
[13] F. Salvan, H. Fuchs, A. Baratoff, and G. Binning, Surf. Sci. **162**, 634 (1985).
[14] T. Hasegawa, K. Takata, S. Hosaka, and S. Hosoki, J. Vac. Sci. Technol. A **8**, 241 (1990).
[15] J. Nogami, A. A. Baski, and C. F. Quate, Phys. Rev. Lett. **65**, 1611 (1990).
[16] T. Takami, D. Fukushi, T. Nakayama, M. Ude, and M. Aono, Jpn. J. Appl. Phys. (to be published).
[17] K. Higashiyama, S. Kono, and S. Sagawa, Jpn. J. Appl. Phys. **25**, L117 (1986).
[18] S. Y. Tong, H. Huang, and C. M. Wei, Phys. Rev. B **46**, 2452 (1992).
[19] C. M. Wei and S. Y. Tong, Surf. Sci. Lett. **274**, L577 (1992).
[20] C. M. Wei, I. H. Hong, P. R. Jeng, S. C. Shyu, and Y. C. Chou, Phys. Rev. B **49**, 5109 (1994).
[21] C. M. Wei, I. H. Hong, and Y. C. Chou, Surf. Rev. Lett. **1**, 335 (1994).
[22] C. M. Wei, I. H. Hong, P. R. Jeng, S. C. Shyu, and Y. C. Chou, Chem. Phys. Lett. **228**, 513 (1994).
[23] I. H. Hong, P. R. Jeng, S. C. Shyu, Y. C. Chou, and C. M. Wei, Surf. Sci. Lett. **312**, L743 (1994).
[24] J. G. Tobin, G. D. Waddill, Hua Li, and S. Y. Tong, Phys. Rev. Lett. **70**, 4150 (1993).
[25] H. Wu, G. J. Lapeyre, H. Huang, and S. Y. Tong, Phys. Rev. Lett. **71**, 251 (1993).
[26] See, for example, S. Y. Tong, Hua Li, and H. Huang, Surf. Rev. Lett. **1**, 303 (1994).
[27] S. Y. Tong, C. M. Wei, T. C. Zhao, H. Huang, and Hua Li, Phys. Rev. Lett. **66**, 60 (1991).